

Probing the orientation and spatial correlations of dipole fluctuators on the surfaces of ion traps

F. Galve,^{1,*} J. Alonso,^{2,†} and R. Zambrini¹

¹*IFISC (UIB-CSIC), Instituto de Física Interdisciplinar y Sistemas Complejos, Palma de Mallorca, Spain*

²*Institute for Quantum Electronics, ETH Zürich, Otto-Stern-Weg 1, 8093 Zürich, Switzerland*

Trapped-ion quantum platforms are subject to ‘anomalous’ heating due to interactions with electric-field noise sources of nature not yet completely known. There is ample experimental evidence that this noise originates at the surfaces of the trap electrodes, and models assuming fluctuating point-like dipoles are consistent with observations, but the exact microscopic mechanisms behind anomalous heating remain undetermined. Here we show that the normal-mode heating rates of a two-ion system can unveil new information about the underlying noise sources. This is because dipole fluctuators on the electrodes’ surfaces necessarily result in a geometric transition where the heating rates of the normal modes equate. Experimentally-accessible characteristics of this crossover can determine uniquely the mean orientation of the dipoles. The spatial extent of correlations between dipole fluctuators, i.e. the finite sizes of fluctuating patches, can also be determined with two ions. This information can be used to test the validity of candidate microscopic models, which predict correlation lengths spanning several orders of magnitude. Finally, we propose an experiment to measure these effects with currently-available traps and techniques.

PACS numbers:

Trapped atomic ions constitute solid candidates for deployable technologies exploiting the unintuitive properties of quantum mechanics [1, 2]. A number of scalable architectures have been proposed [3–5], but technical constraints limit the current computational power of high-fidelity trapped-ion quantum machines to less than ten qubits [6]. One key aspect towards the most prominent scalable schemes is trap miniaturization. This allows for fast quantum operations on the computational space (internal electronic states) [7, 8] as well as the quantum bus (ions’ motion) [9, 10]. However, trapped-ion experiments suffer from motional heating due to interaction with noise sources of origin not yet completely known [11–13]. The measured effects of this so-called ‘anomalous’ heating scale strongly with the inverse of the ion-electrode distance, posing a major obstacle to trap miniaturization.

Systematic experimental studies suggest that the origin of anomalous heating is due to contaminants on the surfaces of trap electrodes [12]. In [14] the NIST ion-storage group treated electrode surfaces with ion bombardment. The 100-fold reduction in the observed heating rates points at adsorbates as probable culprits for the noise. But recent studies show that this is not the whole picture [15], suggesting that only electrode surfaces subject to radio-frequency drives (as required for ion trapping) are accountable for the heating. This result has a profound impact on the search for possible microscopic models since, to our knowledge, all previous studies considered thermally-driven processes (see [12] for a review of proposed microscopic models). In particular, the diffusion of adsorbates [16–19] is consistent with the most advanced surface-science experiments realized to date on a trap setup [20], appearing to be a plausible mechanism

for anomalous heating.

The elucidation of the origin of noise has been based in studying its scaling for *one ion*, usually assumed as $S_E \sim \omega^{-\alpha} d^{-\beta} T^\gamma$ with d the ion’s distance to the electrode, ω its frequency and T the temperature. For different microscopic models a strong distance scaling $\beta > 3$ is predicted and is consistent with experiments [12, 13], whereas frequency and temperature dependences vary for different models. Here we propose a new way of measuring noise which can give finer details on its microscopic origin.

We show that for a trap holding two or more ions a noise crossover effect must take place: there is a point where the center of mass (COM) and relative motions heating rates equate. This previously unknown crossover occurs when ions are separated by comparable distances from each other (l) and from the trap electrodes (d , see fig. 1). We will show that its characteristics depend not only on the spatial extent of correlations of dipole-dipole fluctuations ξ (or the size of patches), but also on the average orientation of the dipoles. This phenomenon is in stark contrast to that found for an homogeneous environment [21], where the properties of the propagator (anisotropy, resonant manifold, etc.) determine the crossover characteristics.

We derive estimates of the correlation lengths ξ of dipole-dipole fluctuations for different microscopic models in the literature and show that the one-ion noise-level departs from its typical d^{-4} scaling [12] when $d \sim \xi$. Likewise the noise crossover for two ions is shifted to higher ion-ion distances l in this regime. Further, the absence/presence of noise crossover for different motional degrees of freedom uniquely determines the mean orientation of dipoles. As a side result, we show that the effect of dipole orienta-

tions can also be observed with a single ion. This might explain recent results at NIST, where noise levels were measured to be highest for ion motion parallel to the surface projection of the sputter beam at a well-defined angle [22]. Finally, we propose a realistic experiment to measure and characterize the noise crossover. This can be carried out with current state-of-the-art Paul traps and techniques.

Electric field noise.— Every dipole source on the surface of an electrode represents a noisy source of electric potential at the ion position: $\phi(\vec{r}) = \vec{\mu} \cdot \vec{r}/|\vec{r}|^3$, with $\vec{\mu}$ the dipole moment of the ion and \vec{r} the position of the dipole relative to the ion. Heating rates for two ions along a given motional degree of freedom, say x , depend on the correlators $\langle E_x(\vec{r}_i, \tau) E_x(\vec{r}_j, 0) \rangle$, with $E_x(\vec{r}_i, \tau)$ the total electric field component along x at time τ at the ion's position \vec{r}_i . We derive in Appendix A the master equation for two ions in Lindblad form, exhibiting the desired heating rates.

Let us consider two coupled identical ions aligned along the x -axis (see Fig. 1), separated by l from each other and d from the trap electrodes. We will assume in what follows that all relevant modes of motion have been cooled close to their respective ground states. It is convenient to move to a normal-mode picture $x_{\pm} = (x_1 \pm x_2)/\sqrt{2}$, where $x_{1,2}$ are the ions' positions with respect to a lab reference frame. Here, the (+) mode corresponds to the center-of-mass motion (COM) and the (−) mode to relative motion (stretch mode), with eigenfrequencies Ω_{\pm} . The heating rates of the normal modes are given by

$$\Gamma_{\pm} = \frac{e^2}{4m\hbar\Omega_j} S_{\pm}, \quad (1)$$

with e and m the ions' charge and mass respectively, \hbar

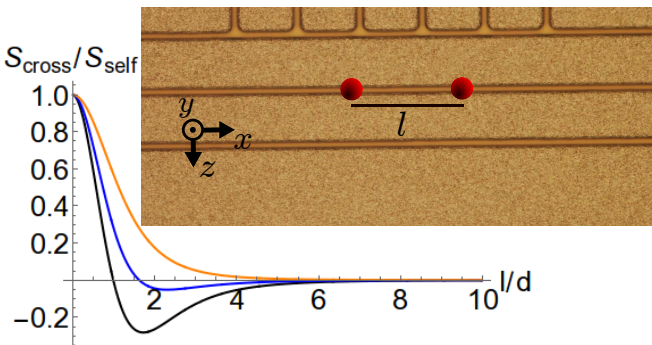


FIG. 1: Ratio $S_{\text{cross}}/S_{\text{self}}$ for the different motional degrees of freedom of a two-ion system: x (black), y (blue) and z (orange). The dipoles are assumed to be uniformly distributed and pointing along y . The electrode-area included in this simulation is a square of side $20d$, which is enough to avoid finite-size effects. Inset: Sketch of a surface-electrode Paul trap with segmented electrodes. The ion-ion distance is l and the ion-electrode distance is d , which is usually similar to the width of the central (horizontal) electrode.

the reduced Planck constant, Ω_j the normal-mode frequencies, and

$$S_{\pm} = 2 \int_{-\infty}^{\infty} d\tau e^{-i\Omega_{\pm}\tau} \langle E_x^{(\pm)}(\tau) E_x^{(\pm)}(0) \rangle. \quad (2)$$

the electric-field fluctuations' spectral densities. The fields acting on the normal modes are a linear combination of the fields seen by the individual ions: $\tilde{E}_x^{(\pm)} = [E_x(\vec{r}_1) \pm E_x(\vec{r}_2)]/\sqrt{2}$. Defining $s_{i,i}(\tau) := \langle E_x^{(i)}(\tau) E_x^{(i)}(0) \rangle$, we can write $S_{\pm} = \int_{-\infty}^{\infty} d\tau e^{-i\Omega_{\pm}\tau} [s_{1,1} + s_{2,2} \pm (s_{1,2} + s_{2,1})]$. Although environmental noise leads to coupling between both normal modes [23], a sufficiently homogeneous electrode guarantees that this coupling is negligible (see Appendix A), leading to independent decay channels for the normal modes. For the two ions, this translates into a *self-noise* for each ion ($S_{1,1}$, $S_{2,2}$) and a *cross-noise* ($S_{1,2}$, $S_{2,1}$). The cross-noise governs the transition from what is known in quantum dissipation literature as a common bath (CB) to separate baths (SB). The former dissipates only the coordinate x_+ and leaves x_- unaffected, whereas the latter yields equal-rate dissipation for both. Regrouping $S_{\text{self}} = (S_{1,1} + S_{2,2})/2$ and $S_{\text{cross}} = (S_{1,2} + S_{2,1})/2$, normal modes (\pm) dissipate as $S_{\pm} = S_{\text{self}} \pm S_{\text{cross}}$. SB occurs (no frozen mode) when $S_{\text{cross}} = 0$, and CB (frozen x_+) when $S_{\text{cross}} = S_{\text{self}}$. We will later show that the 'anti-common' bath (aCB) case where $S_{\text{cross}} = -S_{\text{self}}$ (frozen x_-) is also possible.

The x component of the electric field at a position \vec{r} is given by $E_x(\vec{r}, t) = -\partial_x \phi(\vec{r}) = \sum_i (1/4\pi\epsilon_0)^2 \mu_i(t) g_x(\vec{r}, \vec{r}_i)$, where $g_n(\vec{r}, \vec{r}_i)$ are geometric functions given in Appendix B. Thus, the cross- and self-noise are given by expressions of the form

$$s_{i,j}(\tau) = \sum_{l,k} \frac{\langle \mu_l(t) \mu_k(0) \rangle}{(4\pi\epsilon_0)^2} g_x(\vec{r}_i, \vec{r}_l) g_x(\vec{r}_j, \vec{r}_k) \quad (3)$$

where $\langle \mu_l(t) \mu_k(0) \rangle$ is a correlation function between dipoles l and k . This dipole-dipole correlator features separated temporal and spatial terms for proposed microscopic models [12], so we can approximate it by $\langle \mu_l(t) \mu_k(0) \rangle \simeq s_{\mu}(t) f(\vec{r}_l, \vec{r}_k)$ [38]. Here, f is a spatial correlation profile (it can be a phononic correlation decay in the electrode, a domain function for dipoles in the same patch, etc.) and the approximation is valid if time-fluctuations are similar across the whole surface. Thus, after Fourier integration we will have two main ingredients: the dipole fluctuation spectrum at the eigenfrequencies, $S_{\mu}(\Omega_{\pm})$, and geometric contributions (from f and g). For ions in separate wells the Coulomb coupling is small compared to the eigen-frequencies and $S_{\mu}(\Omega_+) \simeq S_{\mu}(\Omega_-)$. The focus of our work will therefore be on the geometric part.

Noise crossover.— We start by considering the noise characteristics of an electrode containing dipoles which point normal to the surface. This is a typical assumption

even in cases where microscopic details are calculated to a large extent [20]. In order to give a clear picture of the origin of the crossover, let us consider the simplest case: all dipoles are pointing normal to the surface $\vec{\mu}_i = \mu_i \hat{u}_y \forall i$, they are uncorrelated, and we focus on the motional mode along x as a function of l . In this case, the cross-noise is proportional to the sum $\sum_i g_x(\vec{r}_1, \vec{r}_i) g_x(\vec{r}_2, \vec{r}_i)$. In the simplest scenario we can assume the dipoles to be almost homogeneously distributed on the surface and replace the sum by an integral. Noting that (see e.g. [24])

$$g_x(\vec{r}_1, \vec{r}_i) = \frac{d(x_i - x_1)}{((x_i - x_1)^2 + z_i^2 + d^2)^{5/2}},$$

one can see that the integral with respect to z is always finite and positive. However, the integral with respect to the dipole coordinate x has an M shape, meaning that for particular parameters the area enclosed by this shape will vanish (see Appendix C). The crossover originates precisely due to the fact that for a given combination $\{d, l\}$ the cross-noise integral will be zero and the cross-noise changes sign. In figure 2 we see the ratio $S_{\text{cross}}/S_{\text{self}}$ for all three degrees of freedom. When $d \gg l$ we have +1 (CB), and around $d = l$ we have 0 (SB). When $d < l$ we have negative values, which means that the stretch mode dissipates at a rate $S_- = S_{\text{self}} - S_{\text{cross}}$ higher than $S_+ = S_{\text{self}} + S_{\text{cross}}$. The crossover is absent for z -motion (in agreement with figure 27 of [12]), however for x - and y -motion it is present, leading to aCB regime.

One could wonder whether a pure aCB regime is at all possible. We show in Appendix D that for a stylus-trap configuration [25] one can reach $S_{\text{cross}}/S_{\text{self}}$ ratios approaching -1. However, in such a trap at least one of the ions will be necessarily driven by micromotion [26], which could make the aCB regime hard to observe.

Dipole orientation.- Before dealing with possible spatial correlations among dipoles, let us consider what happens when dipoles are not normal to the surface. In that case, since the effective dipole of the ion is given by its displacement from the radio-frequency (RF) null and along its motion, different dipole orientations can cause different noise levels along different directions. These can vary by a factor of six depending on dipole orientation (Appendix E), would be detectable with a one-ion probe, and might be behind recent observations with a single ion at NIST [22]. After treating the electrode surfaces with ion-beam sputtering, they observed that two orthogonal motional degrees of freedom were subject to different noise levels, suggesting a preferential orientation of surface dipoles which could be caused by the generation of gold nanochannels on the treated surfaces.

We will characterize the effects of dipole orientation on two ions in different trap configurations in what follows.

Realistic trap configurations.- In order to sense anomalous heating with two ions, it is convenient to have both ions at RF null zones. This can be achieved in segmented,

linear Paul traps (fig. 1), where trap heights are typically $d \simeq L_z$, with L_z the width of the central axial electrode. The ions can be placed at arbitrary positions along the extent of the linear section L_x , allowing for a tunable inter-ion separation l . In the coming analysis we will use as a reference the setup in [27]. Note that this does not compromise the generality of our results. We will further assume that only RF electrodes are sources of noise. Thus we have two electrodes of length L_x , one of them at positive z with width $L_z \simeq L_x/10$, the other starting at negative $z = -L_z$ of width $2L_z$. These correspond to the upper and lower (long) electrodes in figure 1.

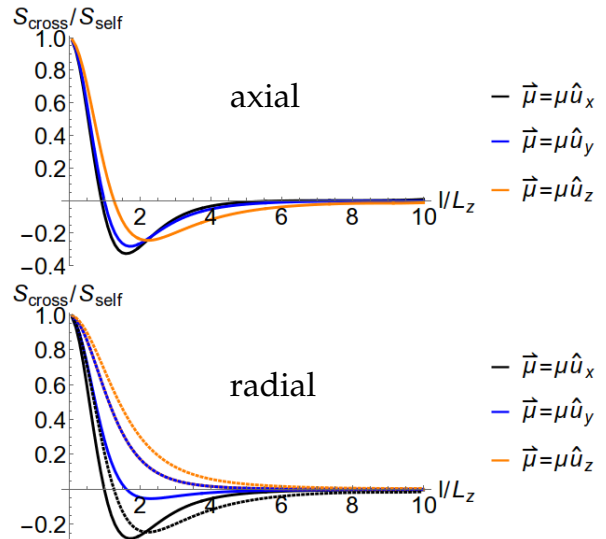


FIG. 2: Ratio of cross- to self-noise for uncorrelated dipoles homogeneously covering the surface of (RF driven) electrodes in the segmented planar trap of ref. [27]. We plot (top) the noise experienced by the axial motion (x), and (bottom) by radial motion along the y (solid) and z (dashed) axes. Note that the dashed blue line and the solid orange line overlap in this plot.

Different dipole orientations result in different dependencies on l of the self- and cross-noise terms (fig. 2). Therefore, experimental measurements of the $S_{\text{cross}}/S_{\text{self}}$ ratio can reveal the mean orientation of the dipole fluctuators. Note that the increased sensitivity of the radial modes as compared to the axial motion render the former as most suitable for this analysis. Table I can be used to gain qualitative insight about the mean orientation of the dipoles. For arbitrary orientations the resulting curves lie between those plotted for the three principal axes, but the structure of crossovers in the table is still valid. For example, any orientation μ_r will keep the $\{\checkmark, \times\}$ signature for any direction $r \neq z$ in the yz -plane, even if the crossover for y -motion is less steep.

Spatial dipole-dipole correlations.- Different microscopic models of dipolar fluctuations result in different two-point spatio-temporal correlation functions $\langle \mu_l(t) \mu_k(0) \rangle \simeq s_\mu(t) f(\vec{r}_l, \vec{r}_k)$, so it is natural to won-

TABLE I: Truth table indicating the presence (\checkmark) or absence (\times) of noise crossover for motion along the y and z axes for a given dipole orientation. This information together with the results of heating-rate measurements of the radial normal modes allow for discrimination of surface-dipole orientations.

Crossover y -motion	Crossover z -motion	Dipole orientation
\checkmark	\checkmark	μ_x
\checkmark	\times	μ_y
\times	\times	μ_z

der whether we can measure its spatial dependence f with our scheme, and thus falsify given models. For one trapped ion we find that the consequence of spatial correlations is the breakdown of the typical d^{-4} scaling for the spectral noise density when $d \lesssim \xi$, tending towards d^{-1} . A simple mean-field argument (see Appendix F) explains the saturation and value of this scaling. For two trapped ions, spatial correlations translate into a shift of the crossover point to higher l/L_z , except for the case of y -motion with μ_x pointing dipoles, where the crossover can even disappear. Importantly, however, these effects are also appreciable only for $\xi \sim L_z$ (see Appendix G). We derive next the size ξ of correlations for several proposed models. For patch models where the dipoles are electronic cloud deformations at the surface due to different crystallographic orientations of domains in the electrode metal, the function f satisfies $f = 1$ whenever two dipoles lie on the same domain and 0 otherwise. Patch sizes in the range [10 nm, 10 μ m] have been measured [28], so ions at distances of tens of microns could potentially feel effects of big enough patches. Another proposed model is based on adatoms (or molecules) stuck to the electrode surface with their induced dipole fluctuating through phononic thermal noise [29]. In such model the dipoles of two adatoms would be spatially correlated through a phonon manifold resonant with their motional bound states (≈ 300 GHz for Neon on Gold) [29]. Taking the dispersion relation of gold (≈ 5 THz at $\lambda \approx 21$ pm, [30]), such frequency would correspond to wavelengths ~ 1 nm. This indicates that correlations would decay at distances ξ on the order of nano-meters, possibly of ~ 100 nm for heavier adsorbed molecules, still far away from the scale of tens of microns. If we assume that dipole fluctuations are RF-driven [15], then a drive at ~ 100 MHz would correspond to wavelengths of ~ 1 μ m (provided a viable mechanism relating RF and phonon excitations exists). For the model of adatoms diffusing on the surface, the spatial scale for dipole-dipole correlations is $\sqrt{D/\Omega_{\pm}}$, with D the diffusion constant. Considering a range $D \in [10^{-14}, 10^{-10}]$ m²/Hz, and frequencies of order MHz, we obtain $\xi \lesssim 1$ nm.

We can thus conclude that within the reach of current distance scales in trap setups, it will be hard to observe the predicted effects of correlations, unless patch noise is

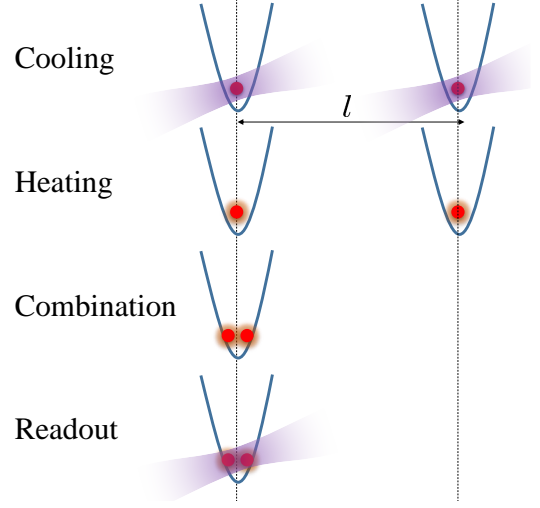


FIG. 3: Experimental sequence to determine the correlation length of the radiative noise sources leading to ‘anomalous’ heating of the motional states of ions in a linear trap. The four radial normal modes of motion of a two-ion system are first cooled close to the ground state [31]. After being exposed to interactions with the environment, the ions are combined in a common potential well, where the motional states of all four modes are read by coupling to the internal electronic states [32].

the correct origin of anomalous heating.

Experimental proposal.— In what follows we present an experimental routine designed to measure the noise crossover from radiative sources on the surfaces of ion-trap electrodes (Fig. 3). With two ions, a straightforward approach is to measure the heating rate Γ_{\pm} of the different normal modes as a function of the distance l between the ions, while keeping the ion-electrode separation d constant. From equation (1) we obtain the noise spectral densities S_{+} and S_{-} , and from them we calculate $S_{\text{self}} = (S_{+} + S_{-})/2$ and $S_{\text{cross}} = (S_{+} - S_{-})/2$. As explained earlier, for the pure CB case the noise ratio $S_{\text{cross}}/S_{\text{self}} = 1$, and only the COM mode will heat up; for pure aCB $S_{\text{cross}}/S_{\text{self}} = -1$, only the relative motion heats up; for SB $S_{\text{cross}}/S_{\text{self}} = 0$, they will both get excited according to the spectral noise-density present at the modes’ frequencies. Such an experiment can be carried out in a linear trap, where radial modes are orthogonal to the trap axis. In our scheme, the heating rates of the radial COM and rocking modes are measured for different ion separations. The plots in Fig. 2 show that an interesting range for the ratio l/d goes from 0.5 to 10 – throughout this range the noise ratio varies strongly in all the cases we have simulated. For an ion-trap height $d = 50$ μ m we should therefore be able to vary l from 25 to 500 μ m. Unfortunately, with realistic experimental parameters the coupling rates between the motional modes of two ions spaced by 500 μ m cannot be expected to exceed ~ 1 Hz [33], making it impossible to spectrally

resolve the normal modes at mega-hertz frequencies. One way of overcoming this limitation is to let the ions heat up while separated and then bring them together to the same potential well to determine the normal-mode states, as in Fig. 3. Ion-chain splitting and recombination operations have been successfully carried out with negligible effects on the radial degrees of freedom [34]. When the ions crystallize in the same trap, the normal modes are easily resolvable [26].

In order to resolve the relevant features in figure 2 it suffices with an absolute uncertainty of the $S_{\text{cross}}/S_{\text{self}}$ ratio $\delta S_{\text{ratio}} \lesssim 0.1$. Assuming a relative uncertainty $\delta\Gamma_+/\Gamma_+ = \delta\Gamma_-/\Gamma_- = \epsilon$ on the determination of the normal-mode heating-rates, as well as no correlations between $\delta\Gamma_+$ and $\delta\Gamma_-$, we find that $\delta S_{\text{ratio}} = \epsilon\sqrt{1 + S_{\text{ratio}}^2 \frac{\sqrt{\Gamma_+^2 + \Gamma_-^2}}{\Gamma_+ + \Gamma_-}} \leq \epsilon\sqrt{2}$. With uncertainties $\epsilon \lesssim 5\%$, which are experimentally feasible, we expect the crossovers predicted in table I to be clearly resolvable.

We have shown above how the noise ratio may vary along different motional directions on the plane of the electrodes. As mentioned before, directionality effects have been observed after treating electrode surfaces with ion bombardment with a well-defined angle, and might be indicative of the microscopic origin of the noise sources [22]. Our scheme is sensitive to such anisotropy, which would lead to measurable differences in the spectral noise densities for the different radial axes.

Discussion.- Microscopic models for anomalous heating are based on dipolar sources with different characteristics: frequency scalings have been a major concern to distinguish among them, but insufficient attention has been paid to their geometric characteristics. Here we find that the normal-mode heating-rates of two ions experience a previously unknown crossover that can be used to distinguish mean dipole orientations and dipole-dipole

correlations (or patch sizes). We provide estimates of the latter for well known models in the literature and show their effect for one- and two-ions configurations. We also propose an experiment which is feasible with current state-of-the-art setups. The idea of exploring spatial characteristics of the noise with more than one ion is left as a new tool for future investigations, and has interesting consequences. For example, in a coupled chain of N ions (see Appendix H) the most noise-resistant normal modes are odd ones, and should be the ones used as quantum information buffers. Further, the availability of many normal modes could potentially give finer details on geometric features of dipole arrangements and correlations.

Acknowledgments.- JA thanks Dustin Hite for discussions. This work has been supported by the EU through the H2020 Project QuProCS (Grant Agreement 641277), by MINECO/AEI/FEDER through projects NoMaQ FIS2014-60343-P, QuStruct FIS2015-66860-P and EPheQuCS FIS2016-78010-P. The research is partly based upon work supported by the Office of the Director of National Intelligence (ODNI), Intelligence Advanced Research Projects Activity (IARPA), via the U.S. Army Research Office grant W911NF-16-1-0070. The views and conclusions contained herein are those of the authors and should not be interpreted as necessarily representing the official policies or endorsements, either expressed or implied, of the ODNI, IARPA, or the U.S. Government. The U.S. Government is authorized to reproduce and distribute reprints for Governmental purposes notwithstanding any copyright annotation thereon. Any opinions, findings, and conclusions or recommendations expressed in this material are those of the author(s) and do not necessarily reflect the view of the U.S. Army Research Office.

Appendix A: Lindblad equation for 2 and N ions

Expanding the interaction Hamiltonian $q\phi(\vec{R})$ as in Appendix B around $\vec{r} = \{0, d, 0\}$ (with the ion quantum fluctuations around that position $\delta\vec{r}$) yields $H = \delta\vec{r} \cdot \vec{\nabla}\phi(\vec{r}) = -\delta\vec{r} \cdot \vec{E}(\vec{R})$. Let us concentrate for simplicity on the interaction (and resultant noise) along x and drop the δ ; thus the interaction energy for two ions is $H_I = -x_1 E_x(\vec{r}_1) - x_2 E_x(\vec{r}_2)$, and similarly for N ions we have $\sum_{i=1}^N x_i E_x(\vec{r}_i)$. We assume that in general the ions are coupled by direct Coulomb interaction, so they will form a set of N normal modes $Q_i = \sum_j f_{i,j} x_j$ with eigenfrequencies Ω_i . Any perturbative noise calculation that we do must be referred to that eigenset (see [23]). Let us rewrite the interaction Hamiltonian

$$H_I = -\sum_{i=1}^N x_i E_x(\vec{r}_i) = -\sum_{i=1}^N \sum_{j=1}^N (f^T)_{i,j} Q_j E_x(\vec{r}_i) = -\sum_{j=1}^N \tilde{E}_x^{(j)} Q_j, \quad (4)$$

with the new ‘electric noises’ $\tilde{E}_x^{(j)} = \sum_{i=1}^N f_{j,i} E_x(\vec{r}_i)$, and where we have used the fact that the transformation matrix f to normal modes is orthogonal (the inverse is its transpose). In the interaction picture the system variables Q_j rotate as

$$\sqrt{\frac{\hbar}{2m\Omega_j}} (A_j e^{-i\Omega_j t} + A_j^\dagger e^{i\Omega_j t}) \quad (5)$$

and we can already calculate heating rates in two ways: either we use the usual argument of obtaining the probability to jump from $|0\rangle$ to $|1\rangle$ in the Fock basis of a given eigenmode, *or* we obtain a master equation for the set of eigenmodes. The first one assumes ground state cooling, while the second is generic.

The *first approach* yields (see e.g. appendix A in [12]) a heating rate for each eigenmode

$$\Gamma_{0 \rightarrow 1}^{(j)} := \Gamma_j = \frac{e^2}{4m\hbar\Omega_j} S_E(\Omega_j),$$

with

$$S_E(\Omega_j) = 2 \int_{-\infty}^{\infty} d\tau e^{-i\Omega_j\tau} \langle \tilde{E}_x^{(j)}(\tau) \tilde{E}_x^{(j)}(0) \rangle.$$

The correlator can be expanded

$$\langle \tilde{E}_x^{(j)}(\tau) \tilde{E}_x^{(j)}(0) \rangle = \sum_{k,l} f_{j,k} f_{j,l} \langle E_x(\vec{r}_k, \tau) E_x(\vec{r}_l) \rangle.$$

In the case of two ions the matrix f is

$$f = \frac{1}{\sqrt{2}} \begin{pmatrix} 1 & 1 \\ 1 & -1 \end{pmatrix}$$

or simply, $\tilde{E}_x^{(\pm)} = [E_x(\vec{r}_1) \pm E_x(\vec{r}_2)]/\sqrt{2}$, with $+/-$ corresponding to center of mass/stretch modes, and also to $Q_{1/2}$, as intuition tells. Finally, the noise kernels suffered by center of mass and stretch modes are

$$\langle \tilde{E}_x^{\pm}(\tau) \tilde{E}_x^{\pm}(0) \rangle = \frac{1}{2} [\langle E_x(\vec{r}_1, \tau) E_x(\vec{r}_1, 0) \rangle + \langle E_x(\vec{r}_2, \tau) E_x(\vec{r}_2, 0) \rangle \pm \langle E_x(\vec{r}_1, \tau) E_x(\vec{r}_2, 0) \rangle \pm \langle E_x(\vec{r}_2, \tau) E_x(\vec{r}_1, 0) \rangle], \quad (6)$$

which can be seen to consist of a *self-damping* part (first two terms) and a *cross-damping* part (last two terms).

In the *second approach*, the dissipator for the Lindblad equation [23] is

$$D(\rho) = \sum_{\omega} \sum_{\alpha, \beta} \gamma_{\alpha, \beta}(\omega) \left(A_{\beta} \rho A_{\alpha}^{\dagger} - \frac{1}{2} \{ A_{\alpha}^{\dagger} A_{\beta}, \rho \} \right) \quad (7)$$

with ω spanning Ω_{\pm} and $A_{\alpha} = A_{+}, A_{-}, A_{+}^{\dagger}, A_{-}^{\dagger}$ are the COM and stretch modes' ladder operators. The basic difference with the previous approach is that, in addition to the (correctly predicted) heating rates Γ_j written above, there appear now cooling rates too, *but also* cross-heating and cross-cooling rates which are neglected in the previous approach. The appearance of cooling is obvious from the time-symmetry of the evolution, but we need not care about it since we are interested in an experimental routine where we cool the normal modes at the beginning of each experimental run.

Interestingly, and sometimes overlooked in the literature, there are cross-terms in the dissipator which couple the normal modes, with kernels of the type

$$\langle \tilde{E}_x^{+}(\tau) \tilde{E}_x^{-}(0) \rangle = \frac{1}{2} [\langle E_x(\vec{r}_1, \tau) E_x(\vec{r}_1, 0) \rangle - \langle E_x(\vec{r}_2, \tau) E_x(\vec{r}_2, 0) \rangle + \langle E_x(\vec{r}_2, \tau) E_x(\vec{r}_1, 0) \rangle - \langle E_x(\vec{r}_1, \tau) E_x(\vec{r}_2, 0) \rangle] \quad (8)$$

which for a sufficiently homogeneous sample will cancel out the first two terms and the last two terms, respectively. If this is fulfilled, the Lindblad dissipator separates into two independent dissipation channels, one for each normal mode. Thus finally, the first approach seems to be sufficient if we consider ground state cooled normal modes, and that the electrode is more or less homogeneously (though random microscopically) populated by adsorbed atoms.

Uncoupled ions.- In the proposed experimental implementation we cool the motion of two ions separated by l , where they can be only weakly coupled. If heating is slow as compared to this separation process we can assume that heating occurs for uncoupled ions, which is the case we consider next. In that case the dissipator for the Lindblad equation [23] is

$$D(\rho) = \sum_{\omega} \sum_{\alpha, \beta} \gamma_{\alpha, \beta}(\omega) \left(a_{\beta} \rho a_{\alpha}^{\dagger} - \frac{1}{2} \{ a_{\alpha}^{\dagger} a_{\beta}, \rho \} \right)$$

with $\alpha, \beta = a_1, a_2, a_1^\dagger, a_2^\dagger$ the usual creation-annihilation operators for the axial ions motion. This dissipator can be diagonalized in the basis $a_\pm = (a_1 \pm a_2)/2$, if we have $\gamma_{1,1} = \gamma_{2,2} \hat{=} \gamma_{\text{self}}$. It yields independent dissipation for the C.O.M. and stretch modes, as was expected by symmetry (*i.e. as before but the Lindbladian does not couple center of mass and stretch modes*). Respectively they dissipate with $\gamma_\pm = \gamma_{\text{self}} \pm \gamma_{1,2}$. These coefficients are again the Fourier transform of the time-correlation functions

$$\gamma_{\alpha,\beta}(\omega) = \mathcal{F}(\langle E_x(\vec{r}_\alpha, t) E_x(\vec{r}_\beta) \rangle) \quad (9)$$

Summary.- All this elaborate discussion was intended to show all the pitfalls that exist when considering the generic problem of a coupled two-body dissipative system, which after assuming enough homogeneity of the problem, similar normal modes' frequencies and ground-state cooled modes, allows us to arrive to an intuitive result: whenever we have that 'cross' $\sim \langle E_x(\vec{r}_1, t) E_x(\vec{r}_2, 0) \rangle$ is similar to 'self' $\sim \langle E_x(\vec{r}_1, t) E_x(\vec{r}_1, 0) \rangle = \langle E_x(\vec{r}_2, t) E_x(\vec{r}_2, 0) \rangle$, we will have what is normally called a *common bath* or a spatially-correlated environment, and the stretch mode will not dissipate. Note also that the sign of the cross term is very important: if it is positive it will induce higher dissipation for the COM, while when negative the stretch will suffer more.

Hence, we call for short (in analogy with common-use nomenclature)

$$S_{\text{cross}} = \frac{1}{2}(\langle E_x(\vec{r}_1, t) E_x(\vec{r}_2, 0) \rangle + \langle E_x(\vec{r}_2, t) E_x(\vec{r}_1, 0) \rangle) \quad S_{\text{self}} = \frac{1}{2}(\langle E_x(\vec{r}_1, t) E_x(\vec{r}_1, 0) \rangle + \langle E_x(\vec{r}_2, t) E_x(\vec{r}_2, 0) \rangle) \quad (10)$$

and compare their magnitudes and relative sign in the main text.

Appendix B: Dipole geometric functions

The spatial functions describing the interaction of one dipole $\vec{\mu}$ with the ion motion in a given axis are given here. Noting that the ion is at $\vec{r} = \{x, y, z\}$ (fluctuating close to the point $\{0, d, 0\}$), the dipole is at $\vec{r}_d = \{x_d, 0, z_d\}$, the distance is defined as $\vec{R} = \vec{r} - \vec{r}_d$ and the electric potential between both is

$$\phi = \frac{1}{4\pi\epsilon_0} \frac{\vec{\mu} \cdot \vec{R}}{|\vec{R}|^3}$$

we can easily obtain the total electric field in any direction $\vec{E} = -\vec{\nabla}\phi$. To obtain the noise felt by the ion in one of its eigenmotions, axial or radial, we need to calculate the corresponding component of that electric field; we will also write down the expressions when assuming that the dipoles are pointing *only* along a given direction. We define the dipole functions as $g_n(\vec{r}) = -(4\pi\epsilon_0/|\vec{\mu}|)\partial_n\phi(\vec{r})$, after expanding the potential around $\vec{r} \simeq \{0, d, 0\}$:

Noise along x motion:

$$\begin{aligned} g_x(\vec{r}) &= \frac{d^2 - 2x_d^2 + z_d^2}{(d^2 + x_d^2 + z_d^2)^{5/2}} \quad , \quad \vec{\mu} = \mu\hat{u}_x \\ g_x(\vec{r}) &= \frac{3dx_d}{(d^2 + x_d^2 + z_d^2)^{5/2}} \quad , \quad \vec{\mu} = \mu\hat{u}_y \\ g_x(\vec{r}) &= -\frac{3x_d z_d}{(d^2 + x_d^2 + z_d^2)^{5/2}} \quad , \quad \vec{\mu} = \mu\hat{u}_z \end{aligned}$$

Noise along y motion:

$$\begin{aligned} g_x(\vec{r}) &= \frac{3dx_d}{(d^2 + x_d^2 + z_d^2)^{5/2}} \quad , \quad \vec{\mu} = \mu\hat{u}_x \\ g_x(\vec{r}) &= -\frac{2d^2 - x_d^2 - z_d^2}{(d^2 + x_d^2 + z_d^2)^{5/2}} \quad , \quad \vec{\mu} = \mu\hat{u}_y \\ g_x(\vec{r}) &= \frac{3dz_d}{(d^2 + x_d^2 + z_d^2)^{5/2}} \quad , \quad \vec{\mu} = \mu\hat{u}_z \end{aligned}$$

Noise along z motion:

$$\begin{aligned} g_x(\vec{r}) &= \frac{-3x_d z_d}{(d^2 + x_d^2 + z_d^2)^{5/2}} \quad , \quad \vec{\mu} = \mu \hat{u}_x \\ g_x(\vec{r}) &= \frac{3d z_d}{(d^2 + x_d^2 + z_d^2)^{5/2}} \quad , \quad \vec{\mu} = \mu \hat{u}_y \\ g_x(\vec{r}) &= \frac{d^2 + x_d^2 - 2z_d^2}{(d^2 + x_d^2 + z_d^2)^{5/2}} \quad , \quad \vec{\mu} = \mu \hat{u}_z \end{aligned}$$

In the case of 2 ions, their positions will now be $\vec{r}_1 = \{-l/2, d, 0\}$ and $\vec{r}_2 = \{l/2, d, 0\}$ and we can use the former expressions by substituting $x_d \rightarrow x_d \pm l/2$ respectively.

Appendix C: Origin of cross-noise vanishing

We have argued that the cross-noise vanishes for some ion motions and dipoles orientations. Let us take for example motion along x and dipoles pointing normal to the electrode ($\vec{\mu} = \mu \hat{u}_y$). Considering for the moment a collection of uncorrelated, homogeneously distributed dipoles, we have that the cross-noise of two ions sitting at $\{-l/2, d, 0\}$ and $\{l/2, d, 0\}$ is proportional to

$$\frac{(x_d - l/2)(x_d + l/2)}{(d^2 + z_d^2 + (x_d - l/2)^2)^{5/2}(d^2 + z_d^2 + (x_d + l/2)^2)^{5/2}}.$$

Integrating this function along z_d yields always a finite value, however the behavior along x_d is like an M, as seen in figure 4 (left). The area enclosed by this curve can be positive, negative or zero depending on the ratio d/l , with the change of sign occurring near $d = l$. For other directions of motion and dipole orientations, using the functions $g_n(\vec{r})$

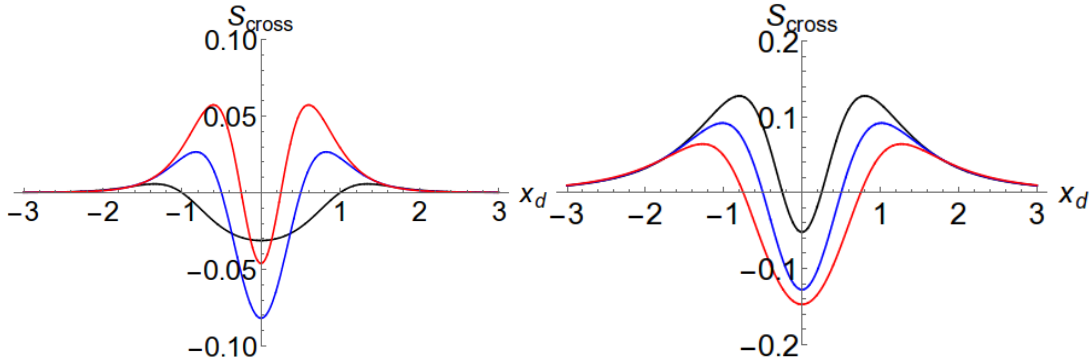


FIG. 4: (Left) Spatial dependence of cross-noise for x motion and dipoles oriented along y . (Right) Same plot for monopolar sources. Depending on the ratio $l/d = 2, 1, 0.5$ (black, blue, red) the shape enclose a negative, null or positive area, whence the noise crossover behavior.

given in Appendix B, it is easy to deduce the properties that we have summed up in figure 2 and Table I.

What about monopolar charges? In that case, the electric potential $\phi \propto 1/|\vec{R}|$ is even (instead of odd) under reflection $\vec{R} \rightarrow -\vec{R}$. Still in this case, we have a crossover, see figure 4 (right). Take as before x -motion and dipoles along y , the cross-noise is here proportional to

$$\frac{(x_d - l/2)(x_d + l/2)}{(d^2 + z_d^2 + (x_d - l/2)^2)^{3/2}(d^2 + z_d^2 + (x_d + l/2)^2)^{3/2}},$$

which is the same as above only that instead of $5/2$ we have $3/2$ exponents. The difference in crossover is that for monopoles it occurs at $l/d \simeq 2$.

Appendix D: Pure anti-common bath regime

It is intuitive that when two coupled units are close to each other and far away from a noisy environment they will experience a common bath (CB), and this is what has been predicted in the main text. But, what about the

opposite, is there a regime where the stretch mode is the only dissipative degree of freedom? In the main text figures we have seen that the minimum $S_{\text{cross}}/S_{\text{self}}$ was around -0.4 . We investigate this in figure 5 for two geometries: a square finite electrode, and a stylus trap as in [15]. For the square electrode a value of almost -1 is reached around $\{d, l\} = \{1.2L_x, 1.4L_x\}$. A value lower than -0.9 is reached $\{d, l\} \simeq \{L_x, L_x\}$. For the stylus trap a lowest value of $\simeq -0.95$ is reached at reasonable distances $\{d, l\} = \{1.5R, 2R\}$, although the absence of a common RF null for two ions in this configuration might require active stabilization of the RF-drive amplitude, whose noise could otherwise mask anomalous heating.

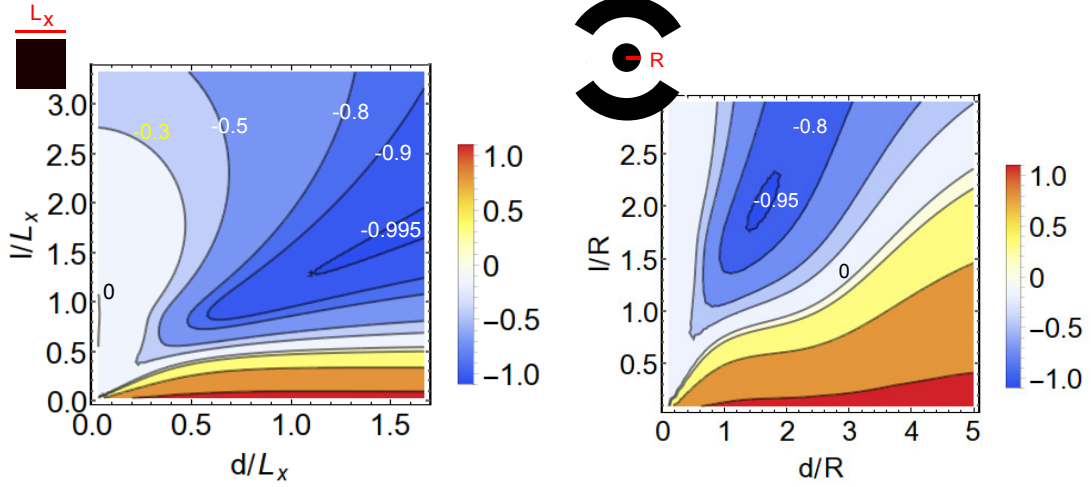


FIG. 5: Noise ratios $S_{\text{cross}}/S_{\text{self}}$ for the x -motion of 2 ions above two different geometries, with homogeneous distribution of dipoles pointing normal to the surface: (Left) square electrode $L_x = L_z$, when the rest of $y = 0$ plane is dielectric (or empty), and (right) a stylus trap as in [15] with inner disk electrode of radius R and an outer ring from $3R$ to $5R$; further apart there are 4 disks, but for the distances considered here they do not affect the ions; the spaces between electrodes act as empty spaces.

Appendix E: 1-ion noise level for different dipole orientations

Dipole-dipole interactions, as that caused by a surface dipole and the displaced charged ion from its equilibrium position, have a preferred direction. It is hence to be expected that different orientations of dipole sources will yield different noise levels even for a 1-ion configuration. Next we plot the simplest situation in which a uniform planar infinite electrode is filled with dipoles oriented along the 3 possible directions: an ion's motion along x feels highest noise levels when dipoles are along \hat{u}_y , while for in-plane dipole orientations, \hat{u}_x produces a noise 4 times higher than \hat{u}_z . The asymmetry between the 3 directions is a direct consequence of the dipole dipole interaction form $3(\vec{m}_1 \cdot \hat{r})(\vec{m}_2 \cdot \hat{r}) - \vec{m}_1 \cdot \vec{m}_2$, with \vec{m}_1 the ion displacement [along \hat{u}_x], \hat{r} the ion-dipole unit vector [along \hat{u}_y] and \vec{m}_2 the dipole moments on the surface.

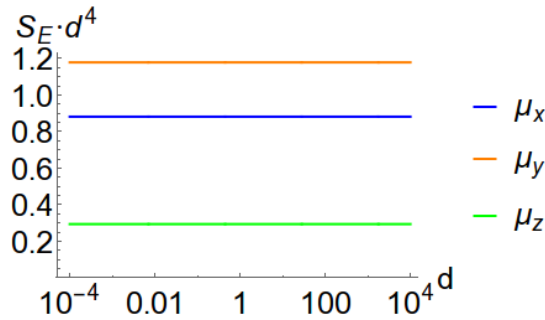


FIG. 6: Noise felt by a single ion in its motion along x when dipoles are pointing in different directions, with an electrode of infinite size arranged as in figure 1. The noise has been normalized by the usual scaling d^{-4} for clarity. The electrode is of infinite size. Noise along the trap axis is clearly dominant.

Appendix F: Mean field dipole

The blurring out into a mean-field dipole in the presence of spatial dipole-dipole correlations can be understood as follows. We can rewrite the noise spectral density seen by 1 ion as the Fourier transform of

$$S = \langle E_x(\tau) E_x(0) \rangle = \sum_{i,j} \left(\frac{1}{4\pi\epsilon_0} \right)^2 \langle \mu_i(t) \mu_k(0) \rangle g_x(\vec{r}_i) g_x(\vec{r}_j) \quad (11)$$

where \vec{r}_i is the distance between dipole i and the ion. As explained in the main text, the spatial-temporal separability of $\langle \mu_i(t) \mu_k(0) \rangle$ allows us to approximate it by $\langle \mu_i(t) \mu_i(0) \rangle f(\vec{r}_i, \vec{r}_j) \simeq S_\mu(t) f(\vec{r}_i, \vec{r}_j)$ where we have assumed that temporal dipole fluctuations are similar for different spatial regions of the electrode, something rather reasonable. Hence, we can write

$$S = \langle E_x(\tau) E_x(0) \rangle \simeq \left(\frac{1}{4\pi\epsilon_0} \right)^2 S_\mu(t) \sum_{i,j} g_x(\vec{r}_i) g_x(\vec{r}_j) f(\vec{r}_i, \vec{r}_j) \quad (12)$$

Further, we can assume that the spatial dipole-dipole correlation profile $f(\cdot)$ is sufficiently translational invariant in the regimes of interest (e.g. ions do not approach too close the borders of electrodes) and thus only depends on the absolute distance between dipoles: $f(\vec{r}_i, \vec{r}_j) \simeq f(|\vec{r}_i - \vec{r}_j|)$. We can sum up the situation by writing the spatial dependence of the spectral noise as

$$\sum_{i,j} g_x(\vec{r}_i) g_x(\vec{r}_j) f(|\vec{r}_i - \vec{r}_j|).$$

If the function f decays significantly for distances greater than ξ as e.g. if $f(\vec{r}_i, \vec{r}_j) = e^{-|\vec{r}_i - \vec{r}_j|/\xi}$, I can define an effective, or ‘mean field’, function $\tilde{g}_x(\vec{r}_i; \xi) := \sum_j g_x(\vec{r}_j) f(|\vec{r}_i - \vec{r}_j|)$ centered at \vec{r}_i and averaged over a size ξ . The noise sum then becomes $\sum_i g_x(\vec{r}_i) \tilde{g}_x(\vec{r}_i; \xi)$, to be compared with the case of uncorrelated dipoles $\sum_i g_x(\vec{r}_i)^2$. Now recall that the g functions are meaningful only in a region of order $\mathcal{A} \sim \mathcal{O}(d)$ around the ion position, so contributions g_x of dipoles far from this spot can be neglected. This allows us to compare the region \mathcal{A}_d of ion-dipoles influence, to the region size \mathcal{A}_ξ defining the averages for the mean-field dipoles. We thus have the following situations:

- $\xi \ll d$ ($\mathcal{A}_d \gg \mathcal{A}_\xi$): Mean-field dipole is seen as an effectively individual dipole and so $\tilde{g}_x(\vec{r}_i; \xi) \rightarrow g_x(\vec{r}_i)$. This is the uncorrelated dipoles case, which is known to scale as d^{-4} .
- $\xi \geq d$: When ξ increases, we reach a point where the averaging region \mathcal{A}_ξ becomes bigger than \mathcal{A}_d , but every dipole lying out of it has a negligible influence on the ion. This means that making ξ bigger yet will not modify the value of the mean-dipole function, which at this ξ *saturates*.

This argument explains why the scaling drops from d^{-4} when $\xi \sim d$ is reached, however it does not explain the new scaling d^{-1} for $d < \xi$. We can, however give an argument why the exponent is less than 4:

When $\mathcal{A}_\xi \geq \mathcal{A}_d$ the sum for the mean-field dipole includes the full region of influence seen by the ion. If we do the brutal simplification $f(|\vec{r}_i - \vec{r}_j|) \simeq 1$ [$\forall i, j \in \mathcal{A}_d$], $\sum_{i,j} g_x(\vec{r}_i) g_x(\vec{r}_j) f(|\vec{r}_i - \vec{r}_j|) \rightarrow \sum_{i \in \mathcal{A}} g_x(\vec{r}_i) \sum_{j \in \mathcal{A}} g_x(\vec{r}_j) = [\sum_{i \in \mathcal{A}} g_x(\vec{r}_i)]^2$ this sum, for dipoles pointing normal to the surface, would yield simply 0 (a constant, i.e. d^0). However if instead of taking $f(|\vec{r}_i - \vec{r}_j|) \rightarrow 1$, we use a linear expansion of the exponential function $f \sim 1 - |\vec{r}_i - \vec{r}_j|/\xi$ the sum yields a scaling d^{-1} as is observed in the next Appendix and is consistent with correlated patch models [36]. It is not obvious that in general the exact resulting exponent should be -1 , but it seems intuitive that the strength of the scaling is tamed.

Further, for the specific case of next appendix [ion motion along x and dipoles pointing along y] we can approximate the dipoles integration as follows: let us take the dipole geometric function from appendix B, which reads

$$g_x(\vec{r}) = \frac{3dx}{(d^2 + x^2 + z^2)^{5/2}}$$

and approximate its biggest contribution which occurs for $\{x, d\} \ll d$ [this approximation usually gives a good estimate of scalings with respect to d],

$$g_x(\vec{r}) \sim 3x/d^4.$$

From now on we will drop numerical factors since we are interested only in the scalings. The noise felt by 1 ion is then dipoles

$$\sum_{i,j} g_x(\vec{r}_i) g_x(\vec{r}_j) f(\vec{r}_i, \vec{r}_j) \sim d^{-8} \sum_{i,j} x_i x_j f(\vec{r}_i, \vec{r}_j).$$

Transforming into integrals we have

$$d^{-8} \int dx \int dx' \int dz \int dz' x x' f(\vec{r}_i, \vec{r}_j).$$

If dipoles are uncorrelated, $f(\vec{r}_i, \vec{r}_j) = \delta(\vec{r}_i, \vec{r}_j)$, and we have $d^{-8} \int dx \int dz x^2$, which gives (recall that the important contribution from dipoles comes from an area of size $\sim d$) d^{-4} as expected.

For the case of very big correlation length ξ , we can expand the exponential

$$d^{-8} \int dx \int dx' \int dz \int dz' x x' \exp(\sqrt{(x-x')^2 + (z-z')^2}/\xi) \sim d^{-8} \int dx dx' dz dz' x x' (1 - \sqrt{(x-x')^2 + (z-z')^2}/\xi)$$

The part with the 1 (as argued above) gives 0 by symmetry, and the rest I can integrate by performing the change of variables $Q_{\pm} = (x \pm x')/\sqrt{2}$ and $Z_{\pm} = (z \pm z')/\sqrt{2}$, so

$$\sim d^{-8} \int dQ_- dQ_+ dZ_- dZ_+ (Q_+^2 - Q_-^2) \sqrt{Q_-^2 + Z_-^2}.$$

A final change of variables for the area enclosed by Z_- and Q_- (of order d) to polar $Q_- = r \cos \phi$, $Z_- = r \sin \phi$, gives

$$\sim d^{-8} \int dQ_+ dZ_+ \int dr d\phi r (Q_+^2 - r^2 \cos \phi) r$$

which after simple integration yields d^{-1} . This highlights the power of approximating the dipole functions in this way.

Appendix G: Modified noise due to correlated dipoles

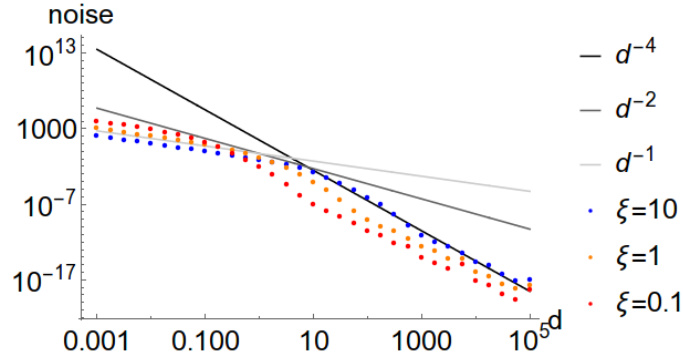


FIG. 7: Noise felt by 1 ion oscillating along x when dipoles in the surface are pointing along y , with spatial dipole-dipole correlation distance ξ . The typical scaling d^{-4} is broken for ion-electrode distances $d < \xi$, where it becomes d^{-1} . [JA - units!]

Here we study what is the effect of a finite extent ξ of spatial dipole-dipole correlations on the characteristics of the noise crossover. For simplicity we take a profile function

$$f(\vec{r}_i, \vec{r}_j) = e^{-|\vec{r}_i - \vec{r}_j|/\xi}$$

although for phononic-induced dipole vibrations of adatoms we should use the more realistic $\text{sinc}(|\vec{r}_i - \vec{r}_j|/\xi)$, and for diffusion of adatoms the Kelvin function $\text{Ker}_0(|\vec{r}_i - \vec{r}_j|/\xi)$. In the case of *one ion* the noise follows, as is well known in the literature [12], a d^{-4} behavior. However, for correlated dipoles, this scaling is modified for $d < \xi$, becoming d^{-1} as can be seen in figure 7.

We plot next the crossover equivalents of figure 2 with correlated dipoles, taking the electrode configuration described in section *Realistic trap configurations*.

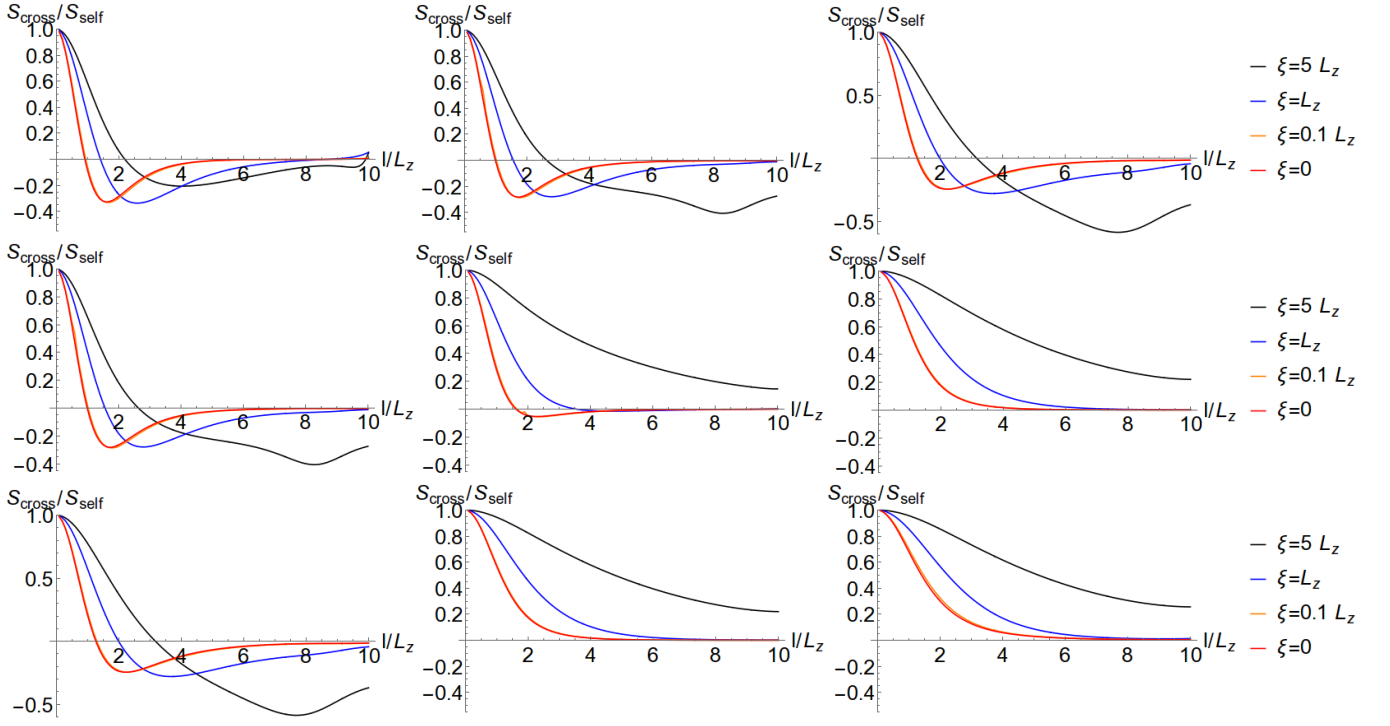


FIG. 8: Noise ratios $S_{\text{cross}}/S_{\text{self}}$ for 2 ions oscillating along x (top), y (middle) and z (bottom), when dipoles in the surface are pointing along x, y, z (left, middle, right). Influence of spatial correlations is noticeable for $\xi > 0.1L_z$.

Appendix H: Chains of coupled ions

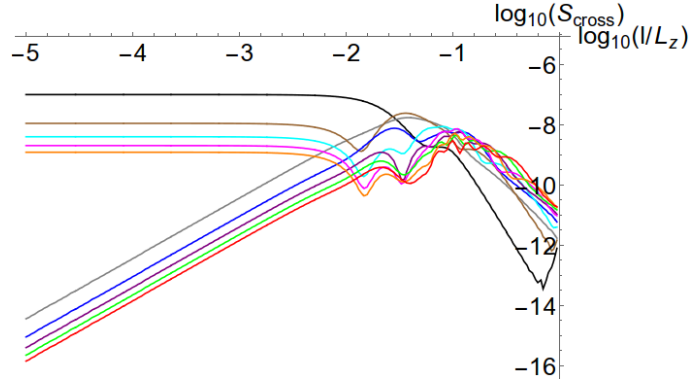


FIG. 9: Cross-noise (arbitrary units) along x -motion for a chain of 10 strongly coupled ions when dipoles in the surface are pointing along x , as a function of the inter-ion distance $l \in [10^{-5}L_z, L_z]$. The electrode has dimensions $L_x = 10L_z$ and the ions are above the electrode at $d = L_z$. Black line is the mode with longest wavelength.

We briefly investigate what happens in a configuration where 10 ions are forming a Coulomb crystal. When they are strongly coupled we expect that normal modes of the chain can divide into sinusoidal waves with 2 kinds of parities: even or odd (under reflection in the center of the chain). It is intuitively expected that even modes will coupled strongly to a CB type of bath, while odds will do so for aCB types of baths. This is precisely what we observe in figure 9: when ions get closer and closer to each other [$d = L_z$, $l \ll L_z$] they begin to see a pure CB configuration, and the noise suffered by odd modes vanishes while for even modes it stays high. Further notice that when $l \simeq L_z$, i.e. when the ion chain almost occupies the full length L_x of the electrode, the mode with longest wavelength (black line) sees the least noise. This is caused by ions being at the point nearest to the aCB regime, and thus the even symmetry of this mode makes it most isolated to noise. These features are of importance for the use of normal modes

as buses for quantum information and for quantum simulations where they provide effective spin-spin interactions among different ions [37].

* Electronic address: fernando@ifisc.uib-csic.es

† Electronic address: alonso@phys.ethz.ch

- [1] J. P. Home *et al.*, Science **325**, 1227 (2009).
- [2] N. M. Linke *et al.*, arXiv:1702.01852
- [3] D. Kielpinski, C. Monroe and D. J. Wineland, Nature **417**, 709 (2002).
- [4] J. I. Cirac and P. Zoller, Nature **404**, 579 (2000).
- [5] B. Lekitsch *et al.*, Sci. Adv. **3**, e1601540(2017).
- [6] S. Debnath, N. M. Linke, C. Figgatt, K. A. Landsman, K. Wright and C. Monroe, Nature **536**, 63 (2016).
- [7] D. Leibfried *et al.*, Nature **422**, 412 (2003).
- [8] C. Ospelkaus *et al.*, Nature **476**, 181 (2011).
- [9] R. Bowler *et al.*, Phys. Rev. Lett. **109**, 080502 (2012).
- [10] A. Walter *et al.*, Phys. Rev. Lett. **109**, 080501 (2012).
- [11] Q. A. Turchette *et al.*, Phys. Rev. A **61**, 063418 (2000).
- [12] M. Brownnutt, M. Kumph, P. Rabl, and R. Blatt, Rev. Mod. Phys. **87**, 1419 (2015).
- [13] Hite, D. A. *et al.*, MRS Bull. **38**, 826. (2013).
- [14] D. A. Hite *et al.*, Phys. Rev. Lett. **109**, 103001 (2012).
- [15] D.A. Hite *et al.*, MRS Advances, pp. 19. (2017).
- [16] R. E. Burgess, Proc. Phys. Soc. London Sect. B **66**, 334 (1953).
- [17] K. M. Van Vliet and E. R. Chenette, Physica (Utrecht) **31**, 985 (1965).
- [18] M. A. Gesley and L. W. Swanson, Phys. Rev. B **32**, 7703 (1985).
- [19] C. Henkel and B. Horowitz, Phys. Rev. A **78**, 042902 (2008).
- [20] E. Kim *et al.*, Phys. Rev. A **95**, 033407 (2017).
- [21] F. Galve *et al.*, Sci. Reps. **7**, 42050 (2017).
- [22] Private communication with D. Hite (2017).
- [23] H. P. Breuer & F. Petruccione, *The Theory of Open Quantum Systems* (Oxford University Press, Oxford, 2003).
- [24] I. Talukdar *et al.*, Phys. Rev. A **93**, 043415 (2016).
- [25] R. Maiwald, D. Leibfried, J. Britton, J. C. Bergquist, G. Leuchs D. J. Wineland, Nat. Phys **5**, 551 (2009).
- [26] D.J. Wineland *et al.*, J. Res. Natl. Inst. Stand. Tech. **103**, 259 (1998).
- [27] K. R. Brown, C. Ospelkaus, Y. Colombe, A. C. Wilson, D. Leibfried and D. J. Wineland, Nature **471**, 196 (2011).
- [28] J. B. Camp, T. W. Darling and R. E. Brown, J. Appl. Phys. **71**, 783 (1992); F. Rossi and G. I. Opat, J. Phys. D **25**, 1349 (1992).
- [29] A. Safavi-Naini, P. Rabl, P. F. Weck and H. R. Sadeghpour, Phys. Rev. A **84**, 023412 (2011)
- [30] J. W. Lynn, H. G. Smith and R. M. Nicklow, Phys. Rev. B **8**, 3493 (1973).
- [31] R. Lechner *et al.*, Phys. Rev. A **93**, 053401 (2016).
- [32] J. Alonso *et al.*, Nat. Comm. **7**, 11243 (2016).
- [33] F N Krauth and J Alonso and J P Home, J. Phys. B: At. Mol. Opt. Phys. **48**, 015001 (2015).
- [34] H. Kaufmann *et al.*, arXiv:1607.03734 (2016).
- [35] D. V. F. James, Appl Phys B **66**, 181(1998).
- [36] R. Dubessy, T. Coudreau and L. Guidoni, Phys. Rev. A **80**, 031402 (2009).
- [37] Ch. Schneider, D. Porras and T. Schaetz, Rep. Prog. Phys. **75**, 024401 (2012).
- [38] Even in cases where it is not spatio-temporal separable (e.g. adatom diffusion), its frequency spectrum is only important at the ion's frequency, which immediately singles out a purely spatial dependence.